Transient Nitronic Acid Formation in the Acid-Catalyzed Decomposition of Nitrobenzofuroxan and Nitrobenzofurazan σ-Adducts in Methanolic Solution. A Kinetic Study

François Terrier,* Guy Ah-Kow, and Alain-Pierre Chatrousse

Laboratoire de Physicochimie des Solutions, UA CNRS 403, ENSCP, 75231 Paris Cedex 05, France

Received March 19, 1985

Kinetic data for the acid-catalyzed and uncatalyzed decomposition of the dioxolane spiro complexes of 7-(2-hydroxyethoxy)-4-nitrobenzofurazan and -benzofuroxan and of the 7,7-dimethoxy complexes of 7-methoxy-4-nitrobenzofurazan and -benzofuroxan have been obtained over a large pH range in methanol. The ring opening of the spiro complexes but not the methoxide ion departure from the dimethoxy adducts is found to be appreciably catalyzed by carboxylic acids. The corresponding Brønsted α coefficients are equal to about 0.5, indicating concerted acid catalysis. At low pH, i.e., pH <5.5, a fast equilibrium protonation of the para-like NO_2 group of the adducts precedes the decomposition process. The pK_a values associated with the ionization of the resulting nitronic acids are all very similar and of the order of 4.2–4.5, as compared with estimated pK_a values of about 1–2 for analogous nitronic acids of picryl σ-complexes. Kinetic data for the formation of the adducts are also reported. The marked differences observed in the rates of formation and decomposition of the similarly stable benzofurazan and benzofuroxan spiro adducts are interpreted in terms of electrostatic effects connected with the presence of the *N*-oxide group in the transition states for the benzofuroxan reactions.

The way that nitro-2,1,3-benzoxadiazoles and their *N*-oxides, commonly known as nitrobenzofurazans and benzofuroxans, respectively, react with nucleophiles is of great interest with respect to understanding the biological properties of these derivatives.[1-3] In a preceding paper, we reported upon the concurrent formation of methoxy adducts **2a** (**2b**) and **3a** (**3b**) in the reaction of methoxide ion with 4-nitrobenzofurazan (**1a**) and 4-nitrobenzofuroxan (**1b**).[4] The greater stability of the adducts **3** relative to the initially formed isomers **2** was attributed to an extensive delocalization of the negative charge through the nitro group para to their sp^3 carbon. In this article, we report our finding that the *gem*-dimethoxy complexes **6** and the spiro complexes **8** are protonated in acidic methanol to form species which are presumably the nitronic acids $\mathbf{6H^+}$ and $\mathbf{8H^+}$. Formation of these acids as transient intermediates in the acid decomposition of **6** and **8** further supports the fundamental role of a paralike nitro group in the stabilization of 4-nitrobenzofurazan and -benzofuroxan adducts. Kinetic and thermodynamic parameters for the formation of the adducts **5**, **6**, and **8** in methanol are also reported.

Results

To carry out a comprehensive thermodynamic and kinetic study of the formation and decomposition of the adducts **6** and **8**, the reactions have been investigated over the pH range of 2–14.68 at 20 °C in methanol. Dilute benzenesulfonic acid solutions, various buffer solutions, and dilute potassium methoxide solutions were used. The buffer solutions were prepared from the same AH-type acids, i.e., carboxylic acids and phenols, as those employed in previous studies,[4,5] and the concentration of the ionic buffer species A^- was varied between 0.001 and 0.01 M. The ionic strength of the buffer solutions as well as that of the benzene sulfonic acid and potassium methoxide solutions was maintained at 0.01 M by adding NaBr as needed. In such conditions, the H^+ concentration of the methanolic solutions could be deduced from the measured activity a_{H^+} of the solvated proton ($[H^+] = a_{H^+}/\gamma_\pm$ with $\gamma_\pm = 0.66$). The pH values are relative to the standard state in methanol.[4,5]

All kinetic experiments were carried out under pseudo-first-order conditions with an excess of the acid, base,

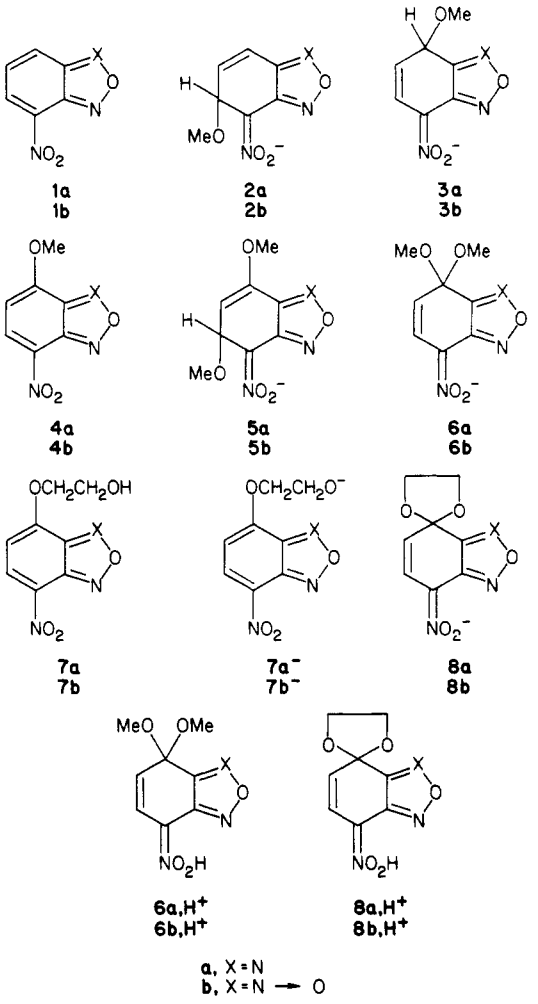

(1) Ghosh, P.; Ternai, B.; Whitehouse, M. W. *Med. Res. Rev.* **1981**, *1*, 159.
(2) (a) Buncel, E.; Chuaqui-Offermans, N.; Norris, A. R. *J. Chem. Soc., Perkin Trans. 1* **1977**, 415. (b) Buncel, E.; Chuaqui-Offermans, N.; Hunter, B. K.; Norris, A. R. *Can. J. Chem.* **1977**, *55*, 2852.
(3) Thompson, S.; Kellicutt, L. *Mutat. Res.* **1977**, *48*, 145.
(4) Terrier, F.; Chatrousse, A. P.; Millot, F. *J. Org. Chem.* **1980**, *45*, 2666.
(5) (a) Terrier, F.; Millot, F.; Morel, J. *J. Org. Chem.* **1976**, *41*, 3892. (b) Terrier, F.; Chatrousse, A. P.; Paulmier, C.; Schaal, R. *Ibid.* **1975**, *40*, 2911.

0022-3263/85/1950-4583$01.50/0

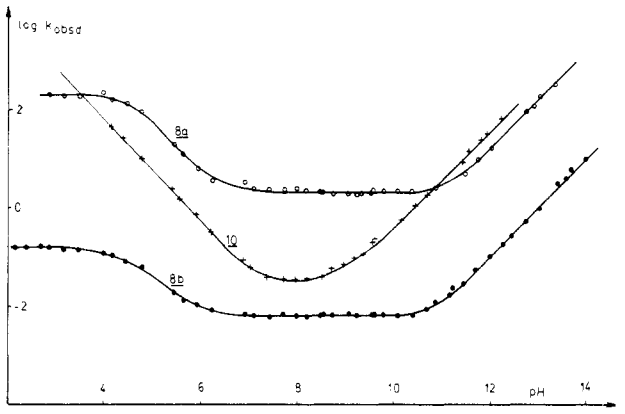

Figure 1. The pH dependence of k_{obsd} (s^{-1}) for the formation and decomposition of the spiro adducts **8a**, **8b**, and **10** in methanol; t = 20 °C; I = 0.01 M.

or buffer reagent over the substrate concentration (~4 × 10^{-5} M). The reactions were monitored spectrophotometrically at the wavelengths corresponding to the absorption maxima of the adducts and/or the ethers.

Spiro Adducts. The formation of **8a** (λ_{max} = 335 nm) and **8b** (λ_{max} = 350 nm) was studied by mixing an aqueous solution of the glycol ethers **7a** (λ_{max} = 350 nm) and **7b** (λ_{max} = 427.5 nm) with buffer solutions at pH >9.5, i.e., cyclohexane carboxylic acid, 2,6-dichlorophenol, 4-cyanophenol, 2-bromophenol buffers, or potassium methoxide solutions in the concentration range 5 × 10^{-4} – 10^{-2} M. Under these conditions, only one single relaxation time was observed. Also, no catalysis by the buffer species could be detected. The k_{obsd} data, which are summarized in Table S1,[6] should fit the eq 1, which reduces to eq 2 be-

$$k_{obsd} = k_{-2} + \frac{Kk_2[CH_3O^-]}{1 + K[CH_3O^-]} \quad (1)$$

$$k_{obsd} = k_{-2} + Kk_2[CH_3O^-] = k_{-2} + \frac{Kk_2K_s}{\gamma_{\pm}a_{H^+}} \quad (2)$$

cause the product $K[CH_3O^-]$ is $\ll 1$ at the pH used.[7-10] The rate and equilibrium constants k_2, k_{-2}, and K refer to the reactions shown in eq 3 which is classical for spiro complex formation in basic media where direct internal cyclization of the glycol side chain (eq 4) is a negligible process.[7-10]

$$7 + CH_3O^- \overset{K}{\rightleftharpoons} 7^- \underset{k_{-2}}{\overset{k_2}{\rightleftharpoons}} 8 \quad (3)$$

$$7 \underset{k_{-1}^{H^+}}{\overset{k_1}{\rightleftharpoons}} 8 + H^+ \quad (4)$$

K_s is the autoprotolysis constant of methanol (pK_s = 16.86 at 20 °C).[11] Reliable values for Kk_2 and k_{-2} were easily obtained from the plateaus and the straight lines of slope +1 in the pH–rate profiles of Figure 1. This allowed us to calculate the stoichiometric equilibrium constants K_c = KK_2 = Kk_2/k_{-2}, values which measure the thermodynamic stability of **8a** and **8b** (eq 5).[7-10] From the KK_2 values thus obtained, the equilibrium constants K_a for adduct formation via eq 4 could be calculated by eq 6.

$$K_c = \frac{[8]}{[7][MeO^-]} = KK_2 = \frac{[8]\gamma_{\pm}a_{H^+}}{[7]K_s} \quad (5)$$

$$K_a = K_c\frac{K_s}{\gamma_{\pm}^2} \quad (6)$$

These K_a values agreed nicely with those directly determined from the pH dependence of the equilibrium absorbances measured at λ = 335 (**8a**) or 427 nm (**8b**) in the pH range of 10–11.5.[10] The results are summarized in Table I.

The breakdown of **8a** and **8b** was studied in the pH range 2–9. The procedure involved the in situ generation of these complexes by placing the parent ethers into a 0.001 M MeOK solution and then mixing this solution with the appropriate buffer or benzenesulfonic acid solution in the stopped flow apparatus. While the experiments performed at pH >5.5 revealed the presence of only one single relaxation effect corresponding to the expected conversion of **8a** and **8b** into **7a** and **7b**, the oscilloscope pictures obtained at pH <5.5 gave evidence for two well-separated processes (Figure S1).[6] The first is associated with an instantaneous spectral change, the intensity of which increases with decreasing pH and reaches a maximum at about pH 3 in the two systems. The second occurs in the same time range as that observed at higher pH and corresponds to the appearance of the parent ethers.

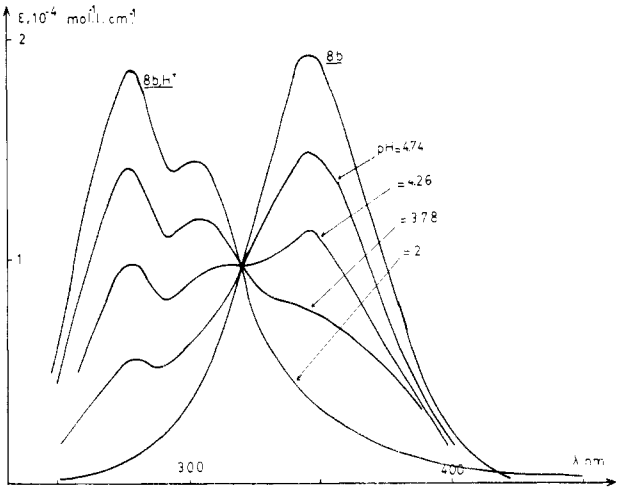

Figure 2. Absorption spectra illustrating the equilibrium protonation of the benzofuroxan spiro adduct **8b** in acidic media in methanol.

Table I. Kinetic and Equilibrium Data for Formation and Decomposition of the Spiro Adducts 8a, 8b, 10, and 11 in Methanol[a]

	8a	8b	10	11[e]
KK_2, M^{-1}	3.79 × 10^5[b] 3.60 × 10^5[c]	6.30 × 10^5[b] 6.31 × 10^5[b]	6.9 × 10^7	3.5 × 10^3
pK_a[f]	10.95	10.70	8.67	12.96
Kk_2, M^{-1} s^{-1}	7.60 × 10^5	3980	1.74 × 10^6	2.5 × 10^4
k_{-2}, s^{-1}	2.10	6.31 × 10^{-3}	0.025[d]	6.5
$k_{-1}^{H^+}K'_a$, s^{-1}	200	0.166		
$k_{-1}^{H^+}$, M^{-1} s^{-1}	3.5 × 10^6	2.92 × 10^3	3.80 × 10^5	
k_1, s^{-1}	3.92 × 10^{-5}	6.84 × 10^{-8}	8.28 × 10^{-4}	
K'_a, M^1	5.73 × 10^{-5}	5.48 × 10^{-5}		
pK'_a	4.24	4.26		

[a] t = 20 °C; I = 0.01 M. [b] KK_2 determined spectrophotometrically. [c] KK_2 calculated from the ratio Kk_2/k_{-2}. [d] k_{-2} calculated from the ratio Kk_2/KK_2. [e] Reference 7c, at 25 °C. [f] pK_a calculated via eq 6.

(6) See paragraph concerning supplementary material at the end of this paper.

(7) (a) Crampton, M. R.; Willison, M. J. *J. Chem. Soc., Perkin Trans. 2*, **1974**, 1681, 1686. (b) *Ibid.* **1976**, 901. (c) Crampton, M. R. *Ibid.* **1973**, 2157.
(8) (a) Bernasconi, C. F.; Gandler, J. R. *J. Org. Chem.* **1977**, *42*, 3387. (b) Bernasconi, C. F.; Howard, K. A. *J. Am. Chem. Soc.* **1982**, *104*, 7248.
(9) Terrier, F. *Chem. Rev.* **1982**, *82*, 77.
(10) Ah-Kow, G.; Terrier, F.; Lessard, F. *J. Org. Chem.* **1978**, *43*, 3578.
(11) Halle, J. C.; Terrier, F.; Schaal, R. *Bull. Soc. Chim. Fr.* **1973**, 37.

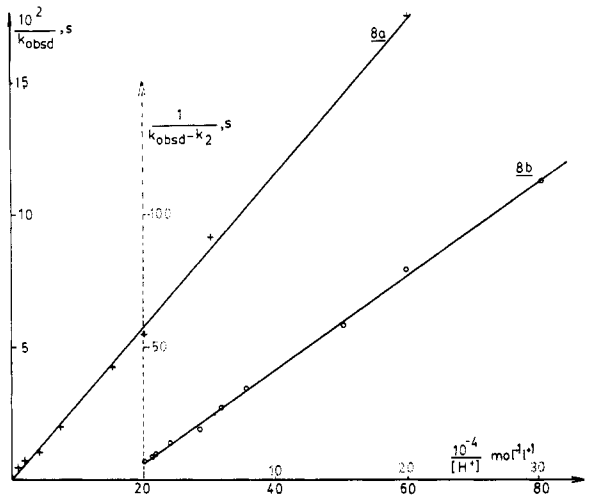

Figure 3. Inversion plots according to eq 9 for the decomposition of the spiro adducts **8a** and **8b** in the pH range 4–5.5 in methanol; t = 20 °C, I = 0.01 M.

Significantly, it was possible to record at different wavelengths and different pH the absorption changes initially observed in the decomposition of the adducts. The results are illustrated by the group of spectra of Figure 2 which refers to the case of **8b**. As can be seen a clean isosbestic point is present at 320 nm, indicating the reversible character of the reaction and suggesting that we are dealing with a fast equilibrium protonation of the adducts. As will be discussed later, there is little doubt that the resulting protonated species which both absorb at $\lambda_{max} \sim 280$ nm are the nitronic acids **8aH⁺** and **8bH⁺**.

Considering the fast initial protonation equilibrium of **8a** and **8b**, the appearance of the ethers **7a** and **7b** in the pH range of 2–9 is described by eq 7, where K'_a is the

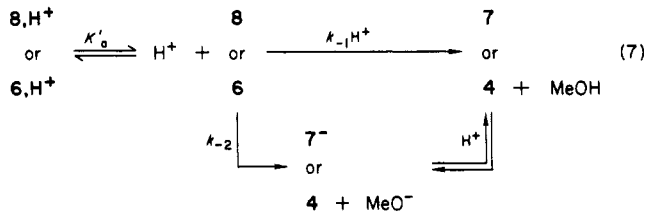

(7)

acidity constant of the protonated adduct while $k_{-1}^{H^+}$ and k_{-2} refer to the H^+-catalyzed and noncatalyzed decomposition of **8a** or **8b**. The values of the observed first-order rate constant k_{obsd} for the process are given in Table S1[6] and fit the eq 8 which accounts for the two limiting situations observed at pH <9 in the pH–rate profiles of Figure 1.

$$k_{obsd} = (k_{-1}^{H^+}[H^+] + k_{-2})\frac{K'_a}{K'_a + [H^+]} \quad (8)$$

(a) At pH >6.5, the k_{-2} pathway is dominant and $K'_a \gg [H^+]$. Thus, $k_{obsd} = k_{-2}$, as previously observed in the pH range 9–10.

(b) At low pH, we have $k_{-2} \ll k_{-1}^{H^+}[H^+]$ and $K'_a \ll [H^+]$ so that $k_{obsd} = k_{-1}^{H^+}K'_a$, accounting for the plateaus observed at pH <3. Since k_{-2} is known with accuracy from the plateau observed at pH >6.5, we have rewritten eq 8 in the form of eq 9 to evaluate the $k_{-1}^{H^+}$ and K'_a values. Using the k_{obsd} values measured between pH 4 and 5.5, inversion plots according to eq 9 were linear (Figure 3).

$$\frac{1}{k_{obsd} - k_{-2}} = \frac{K'_a}{k_{-1}^{H^+}K'_a - k_{-2}}\left(\frac{1}{[H^+]}\right) + \frac{1}{k_{-1}^{H^+}K'_a - k_{-2}} \quad (9)$$

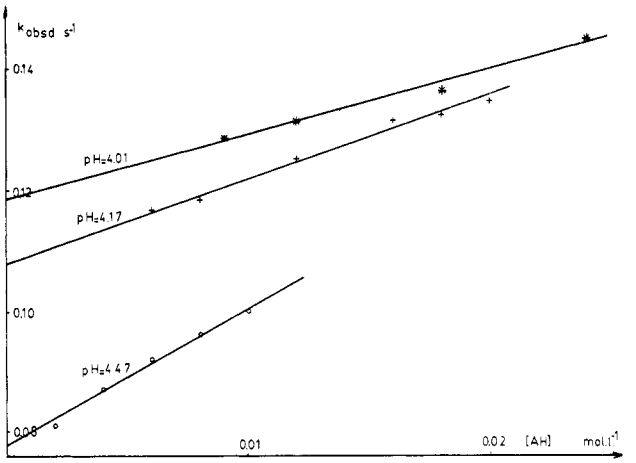

Figure 4. Buffer catalysis of the decomposition of the benzofuroxan spiro adduct **8b** in various trichloroacetic acid buffers in methanol; t = 20 °C, I = 0.01 M.

Table II. Rate Constants k^{AH} for Acid Catalysis of the Ring Opening of the Spiro Complexes 8a, 8b, and 10 in Methanol[a]

buffer acidic species	pK_a	k^{AH}, M^{-1} s^{-1}		
		8a	**8b**	**10**
$CH_3OH_2^+$	−1.4	3.5×10^6	2.92×10^3	3.80×10^5
CCl_3COOH	4.47	1500	4.05	112.2
$CHCl_2COOH$	5.96	285	0.6	29.50
$CH_2ClCOOH$	7.42		0.13	1.49
3-chlorobenzoic acid	8.48			0.50
benzoic acid	9.04			0.35
CH_3OH[b]	17.9	0.085	2.55×10^{-4}	1.01×10^{-3}

[a] t = 20 °C, I = 0.01 M. [b] k^{AH} calculated as $k_{-2}/24.7$.

Combination of the values of the slope and the intercept yields $K'_a = 5.48 \times 10^{-5}$ mol L^{-1} and $k_{-1}^{H^+} = 2.92 \times 10^3$ L mol^{-1} s^{-1} for **8b**. This corresponds to a $k_{-1}^{H^+}K'_a$ value of 0.16 s^{-1}, which is consistent with the observed plateau at pH <3 ($k_{-1}^{H^+}K'_a = 0.166$ s^{-1}). In the case of **8a**, where the intercept was too small to be determined very accurately, the value of the slope was combined with the $k_{-1}^{H^+}K'_a$ = 200 s^{-1} value deduced from the plateau observed in Figure 1. One thus obtains $k_{-1}^{H^+} = 3.5 \times 10^6$ L mol^{-1} s^{-1} and $K'_a = 5.73 \times 10^{-5}$ mol L^{-1}. Combining the $k_{-1}^{H^+}$ values with the K_a values for adduct formation also leads to the k_1 values for direct cyclization of the glycols: k_1(**7a**) = 3.92×10^{-5} s^{-1}; k_1(**7b**) = 5.84×10^{-8} s^{-1}. As expected, these values are very low, confirming that this pathway is negligible in the formation of **8a** and **8b**. The results are summarized in Table I.

Despite the low total buffer concentrations used in our study, i.e., [A^-] + [AH] < 0.05 M, appreciable catalysis by the buffer acid species was observed in the most acidic buffer systems, i.e., chloroacetic acid (pK_a = 7.42), dichloroacetic acid (pK_a = 5.96), and trichloroacetic acid (pK_a = 4.47). This catalysis was studied in detail in working at different constant buffer ratios but different buffer concentrations. In agreement with the rate law of eq 10, all plots of k_{obsd} vs. [AH] at constant pH were linear.

$$k_{obsd} = (k_{-1}^{H^+}[H^+] + k_{-2})\frac{K'_a}{K'_a + [H^+]} + k^{AH}[AH]\frac{K'_a}{K'_a + [H^+]} \quad (10)$$

Significantly, the slopes of these plots were essentially pH independent in the case of the chloroacetic and dichloroacetic buffer systems (Figure S2)[6] where $K'_a/K'_a + [H^+] \sim 1$ but decreased with decreasing pH in the trichloro-

acetic buffers (Figure 4). The various rate constants k^{AH} for catalysis of the breakdown of **8a** and **8b** by AH are listed in Table II. To be noted is that it is the k_{obsd} values extrapolated to zero buffer concentration which have been used to draw the pH–rate profiles of Figure 1 in the pH range 4–7.5.

For the purpose of comparison, the formation and decomposition of the spiro adduct **10** (λ_{max_1} = 480 nm, ϵ = 18 000 M^{-1} cm^{-1}; λ_{max_2} = 417 nm ϵ = 25 000 M^{-1} cm^{-1}) of 1-(2-hydroxyethoxy)-2,4,6-trinitrobenzene (**9**) was studied

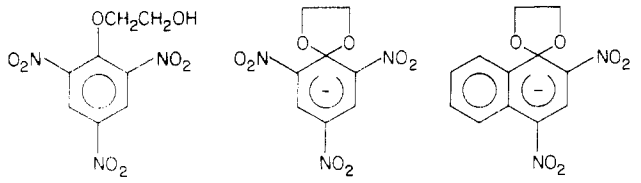

9 **10** **11**

under similar experimental conditions as those used for **8a** and **8b**. Since no evidence for protonation of **10** was found at low pH, the overall k_{obsd}–pH rate profile shown in Figure 1 was analyzed in terms of eq 11. The rate

$$k_{obsd} = \frac{k_{-1}^{H^+} a_{H^+}}{\gamma_\pm} + k_{-2} + k_1 + \frac{Kk_2 K_s}{\gamma_\pm a_{H^+}} \qquad (11)$$

constant Kk_2 for formation of **10** and the rate constant $k_{-1}^{H^+}$ associated with the H^+-catalyzed decomposition of this adduct were easily determined from the straight lines of slope +1 and −1 observed at high and low pH, respectively. In contrast, the rate constant k_{-2} for the noncatalyzed decomposition could not be graphically determined from Figure 1 because the contributions of the $k_{-1}^{H^+}[H^+]$ and/or $Kk_2[CH_3O^-]$ terms are not negligible in the pH range 7–9, where the minimum values of k_{obsd} (Table S2)[6] are observed. Hence, k_{-2} was calculated from the ratio Kk_2/KK_2 by using the value of the equilibrium constant $K_c = KK_2$ for formation of **10**, which was spectrophotometrically determined.

As found for **8a** and **8b**, acid catalysis of the decomposition of **10** was observed and studied in detail in the most acidic buffers. The various rate and equilibrium parameters obtained for **10** as well as those previously reported for the 2,4-dinitronaphthalene analogue **11**[7] are given in Table I and II.

Dimethoxy Adducts. The equilibrium formation of **6a** (λ_{max} = 337 nm, ϵ = 16 000 M^{-1} cm^{-1}) and **6b** (λ_{max} = 345 nm, ϵ = 19 000 M^{-1} cm^{-1}) from the parent ethers **4a** (λ_{max} = 372.5 nm) and **4b** (λ_{max} = 427.5 nm) was studied kinetically in the pH range of 11.8–14.68, using 4-cyano- and 2-bromophenol buffers solutions as well as MeOK [(5 × 10^{-4}–0.01 M] solutions. Under these conditions, no buffer catalysis was detected, and the observed rates (Table S3)[6] nicely obeyed eq 14. This allowed the rate

$$4 + MeO^- \underset{k_{-2}}{\overset{k_2}{\rightleftharpoons}} 6 \qquad (12)$$

$$4 + MeOH \underset{k_{-1}^{H^+}}{\overset{k_1}{\rightleftharpoons}} 6 + H^+ \qquad (13)$$

$$k_{obsd} = k_{-2} + k_2[MeO^-] = k_{-2} + \frac{k_2 K_s}{\gamma_\pm a_{H^+}} \qquad (14)$$

constants k_2 and k_{-2} and the equilibrium constants $K_2 = k_2/k_{-2} = [6][MeO^-]/[4]$ for the reactions shown in eq 12 to be accurately determined. The two limiting situations corresponding to $k_{-2} \gg k_2[MeO^-]$ and $k_{-2} \ll k_2[MeO^-]$ are reflected, respectively, in the plateaus and the straight lines of slopes +1 observed in the pH–rate profiles of Figure 5.

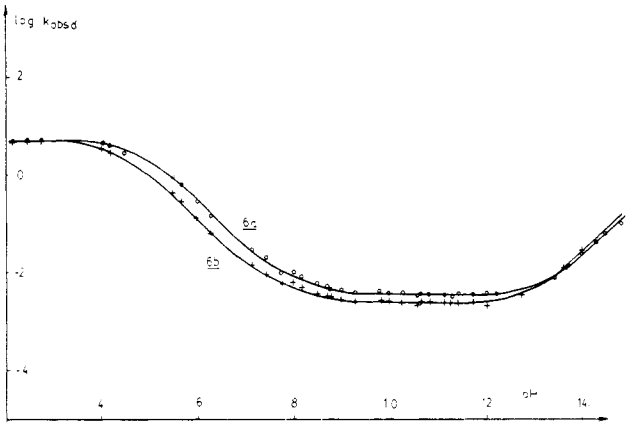

Figure 5. The pH dependence of k_{obsd} (s^{-1}) for the formation and decomposition of the *gem*-dimethoxy adducts **6a** and **6b** in methanol; t = 20 °C, I = 0.01 M.

Although adduct formation through methanol attack on **4a** and **4b** is negligible, the equilibrium constant K_a associated with eq 13 could be calculated from $K_a = K_2K_s/\gamma_\pm^2$.

The decomposition of **6a** and **6b** was studied in the pH range of 2–11.8 using the procedure and the experimental conditions described for **8a** and **8b**. As observed for these latter systems, protonation of the adducts **6a** and **6b** occurs prior to the appearance of the ethers **4a** and **4b** at pH <5.5. The absorption spectra of the resulting nitronic acids **6aH**$^+$ and **6bH**$^+$ which both absorb at ~280 nm are given in Figure S3[6] while the pH dependence of the rates of decomposition is shown in Figure 5. In accordance with the scheme of eq 7, the k_{obsd} data fitted eq 8 very well, allowing an accurate determination of the rate constants $k_{-1}^{H^+}$ for the H^+-catalyzed decomposition of **6a** and **6b** and the acidity constants K'_a of the nitronic acids **6aH**$^+$ and **6bH**$^+$. A noteworthy feature of the decomposition of **6a** and **6b** is that in contrast to the situation with **8a** and **8b**, no catalysis by carboxylic buffer acid species could be detected.

The various rate and equilibrium constants for the formation and decomposition of **6a** and **6b** are summarized in Table III. Also included for comparison are the previously reported kinetic and equilibrium data for formation of the 5,7-dimethoxy isomers **5a** and **5b**, which form prior to **6a** and **6b** at MeO^- concentrations >0.01 M[12] and those for the analogous adducts **12**, **13**, and **14** of 2,4,6-trinitroanisole[14] and 1-methoxy-2,4-dinitronaphthalene.[15,16]

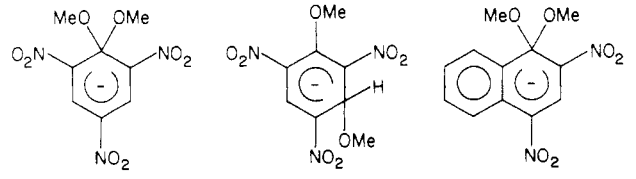

12 **13** **14**

Discussion

Comparison of the equilibrium parameters in Tables I and III shows that the stability of the various 4-nitro-

(12) Ah-Kow, G. C. R. Hebd. Seances Acad. Sci., Ser. C. 1978, 287, 231.
(13) Di Nunno, L.; Florio, S.; Todesco, P. E. J. Chem. Soc., Perkin Trans. 2 1975, 1469.
(14) (a) Bernasconi, C. F. J. Am. Chem. Soc. 1970, 92, 4682. (b) Ibid. 1971, 93, 6975.
(15) Millot, F.; Terrier, F. Bull. Soc. Chim. Fr. 1971, 3897.
(16) Fendler, J. H.; Fendler, E. J.; Byrne, W. E.; Griffin, C. E. J. Org. Chem. 1968, 33, 977.

Table III. Kinetic and Equilibrium Data for Formation and Decomposition of the Various Dimethoxy Adducts in Methanol at t = 20 °C

	6a[a]	6b[a]	12[b]	5a[c,d]	5b[c]	13[b]	14[e]
k_2, M^{-1} s^{-1}	7.58	12.02	11.8	347.2	348	690	0.745
k_{-2}, s^{-1}	3.55×10^{-3}	2.29×10^{-3}	6.05×10^{-4}	9.2	5	290	2.4×10^{-3}
K_2, M^{-1}	2135	5250	19500	37.74	69.6	2.56	310
pK_a[f]	13.17	12.78	12.21				
$k_{-1}^{H^+}K'_a$, s^{-1}	4.85	4.64					
$k_{-1}^{H^+}$, M^{-1} s^{-1}	1.76×10^5	7.94×10^4					
K'_a, M	2.75×10^{-5}	5.84×10^{-5}					
pK'_a	4.56	4.23					

[a] This work at t = 20 °C; I = 0.01 M. [b] Values calculated at t = 20 °C from data in ref 14; I = 0.5 M. [c] Reference 12. [d] At 25 °C: k_2 = 350 M^{-1} s^{-1}, k_{-2} = 16 s^{-1}, K_2 = 22 M^{-1} in ref 13. [e] Reference 15. [f] K_a calculated from $K_a = K_2K_s/\gamma_\pm^2$.

benzofurazan and -benzofuroxan adducts is intermediate between that of the related trinitrobenzene complexes and that of the related dinitronaphthalene complexes. These observations further emphasize the remarkable stability of these heterocyclic σ-adducts, which is a consequence of both the very strong electron-withdrawing character of the furazan and furoxan rings and the low aromaticity of the benzofurazan or benzofuroxan system.[4,9,10,17-21] That the equilibrium constants (KK_2 or K_2) for complex formation are about 2-fold greater for the benzofuroxan (**5b**, **6b**, **8b**) than the benzofurazan (**5a**, **6a**, **8a**) adducts is perhaps unexpected, in view of the idea that the electron-donating effect of the oxygen atom of the *N*-oxide group should partially reduce the overall electron-withdrawing effect of the furoxan ring compared with that of the furazan analogue.[22] However, a similar situation was encountered in comparing the adducts **2a** and **2b** as well as **3a** and **3b** in methanol.[4] In contrast, the spiro complex **8a** is 2.7-fold more stable than its analogue **8b** in aqueous solution.[10] Differences in the solvation of the *N*-oxide group in water and methanol might account for these observed differences in the overall electron-withdrawing effects of the furoxan and furazan rings.

As can be seen in Table III, the similar stabilities of the *gem*-dimethoxy adducts **6a** and **6b** as well as those of the 5,7-dimethoxy isomers **5a** and **5b** are the reflection of similar rates of formation and decomposition. In contrast, the spiro complexes **8a** and **8b** have markedly different rates of formation and decomposition despite their similar thermodynamic stability. Both the Kk_2 and k_{-2} values are more than 10^2 times greater for **8a** than for **8b**: Kk_2(**8a**)/Kk_2(**8b**) = 191; k_{-2}(**8a**)/k_{-2}(**8b**) = 333. Similarly, the rate constant k_1 for direct cyclization of the parent glycols as well as the rate constants $k_{-1}^{H^+}$ and k^{AH} for catalysis of the ring opening of the adducts by H^+ or the general acids AH are much greater for **8a** than **8b**: k_1(**8a**)/k_1(**8b**) = 671; $k_{-1}^{H^+}$(**8a**)/$k_{-1}^{H^+}$(**8b**) = 1200; $k_{-1}^{CHCl_2COOH}$(**8a**)/$k_{-1}^{CHCl_2COOH}$(**8b**) = 475.

In general, it has been found that spiro adducts have a much higher susceptibility to decompose than their *gem*-dimethoxy analogues, and the data for the trinitrobenzene and dinitronaphthalene adducts in Tables I and III are consistent with this observation.[7-10,18] On this basis, our finding that **8a** decomposes much more rapidly than **6a** was to be expected. Instead, the fact that **8b** and **6b** decompose at rather similar rates suggests a somewhat abnormal behavior of the benzofuroxan spiro complex. Since it appears that the rate of formation of **8b** is also abnormal relative to that of **8a**, the situation can be accounted for only in terms of a special effect on the transition state which is not present (or present to a smaller extent) in either the reactants or in the adducts.[8b,23,24] This confirms previous results obtained in aqueous solution and is presumably the reflection of an unfavorable electrostatic interaction between the *N*-oxide group and the approaching or departing glycolate or glycol side chain in the corresponding transition states for the dioxolane ring-closure or -opening processes.[10] Thus, in the transition-state **15**, which refers to the Kk_2 and k_{-2} pathways, electrostatic

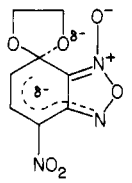

15

destabilization might arise from repulsion between the two negative oxygens. In the case of the glycol reaction, the situation is more difficult to visualize, but the data obtained on the acid-catalysis breakdown of the spiro adducts will support an electrostatic explanation (vide infra).

Nitronic Acid Formation. The most interesting result of this work is undoubtedly our observation that the adducts **6** and **8** are susceptible to fast protonation in acidic methanol. In looking at the resonance structures **16** and **16′** it appears that both the NO_2 group and the 3-nitrogen of the annelated furazan and furoxan rings are possible protonation sites of the adducts. In the case of the ben-

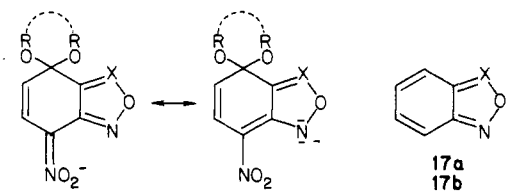

16a **16b** **16a′** **16b′** **17a** **17b**

a, X=N
b, X=N → O

zofuroxan systems, the oxygen atom of the *N*-oxide group is also a potential site of protonation. On this basis, our

(17) Illuminati, G.; Stegel, F. *Adv. Heterocycl. Chem.* **1983**, *34*, 306.
(18) Buncel, E.; Crampton, M. R.; Strauss, M. J.; Terrier, F. In "Electron Deficient Aromatic and Heteroaromatic-Base Interactions"; Elsevier: Amsterdam, Holland, 1984; p 166.
(19) (a) Terrier, F.; Chatrousse, A. P.; Soudais, Y.; Hlaibi, M. *J. Org. Chem.* **1984**, *49*, 4176. (b) Terrier, F.; Halle, J. C.; Pouet, M. J.; Simonnin, M. P. *Ibid.* **1984**, *49*, 4363.
(20) Strauss, M. J.; Renfrow, R. A.; Buncel, E. *J. Am. Chem. Soc.* **1983**, *105*, 2473.
(21) (a) Spear, R. J.; Norris, W. P.; Read, R. W. *Tetrahedron Lett.* **1983**, *24*, 1555. (b) Norris, W. P.; Spear, R. J.; Read, R. W. *Aust. J. Chem.* **1983**, *36*, 297. (c) Read, R. W.; Spear, R. J.; Norris, W. P. *Ibid.* **1984**, *37*, 985.
(22) Harris, R. K.; Katritzky, A. R.; Oksne, S.; Bailey, A. S.; Paterson, W. G. *J. Chem. Soc.* **1963**, 197.
(23) Bernasconi, C. F.; Bergstrom, R. G. *J. Am. Chem. Soc.* **1973**, *95*, 3603.
(24) Kresge, A. J. *Chem. Soc. Rev.* **1973**, *2*, 475.

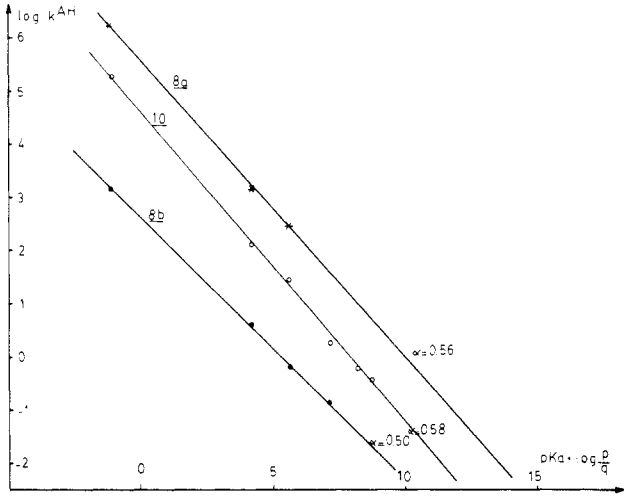

Figure 6. Brønsted plots for the general-acid-catalyzed decomposition of the spiro adducts **8a**, **8b**, and **10** in methanol; t = 20 °C, I = 0.01 M.

proposal that the resulting protonated species are most probably the nitronic acids $\mathbf{6H^+}$ and $\mathbf{8H^+}$ needs to be discussed.

Katritzky et al. have previously shown that the basicity of a number of benzofurazans and benzofuroxans is very low.[25] The pK_a value for protonation of the unsubstituted benzofurazan and benzofuroxan **17a** and **17b** have been estimated to be ~−8.35 from equilibrium studies in concentrated sulfuric acid solutions.[25] This indicates that the basicity of the heterocyclic nitrogen atom in both **17a** and **17b** as well as that of the oxygen atom of the *N*-oxide group in **17b** is very low. In the adducts **6** and **8**, an increase in the charge density of the 3-nitrogen may be expected (see **16** ↔ **16′**), but the effect must be strongly attenuated by the well-known high efficiency of a para nitro group in delocalizing electrons by resonance interaction.[9,18] Indeed, convincing evidence has been previously presented that the annelated furazan and furoxan rings have a much stronger inductive effect but much less capacity for resonance delocalization of charge than a nitro group.[4,26,27] Further illustration of this behavior is provided by a comparison of the equilibrium and rate parameters that we have obtained for the formation of the isomeric adducts **5** and **6**. As can be seen in Table III, both the *gem*-dimethoxy complexes **6a** and **6b** form more slowly but have a greater thermodynamic stability than their 5,7-dimethoxy isomers **5a** and **5b**. Since no important steric factors are operating in the formation of 4-nitrobenzofurazan and -benzofuroxan adducts,[4] the comparison of the resonance structures **16** ↔ **16′** and **18** ↔ **18′** shows clearly that the only way to account for this result is to assume a primary role to the 4-NO_2 group in stabilizing **6a** and **6b**. Accordingly, protonation of these adducts and of their spiro analogues **8a** and **8b** at the NO_2 group to give the nitronic acids $\mathbf{6H^+}$ and $\mathbf{8H^+}$ appears to be the most reasonable process. A noteworthy result is that the pK'_a values measured for the four nitronic acids studied are similar. This is however in accord with the idea that the nature of the moiety(-ies) bonded to the sp^3 carbon has no major influence on the delocalization of the negative charge through the NO_2 group in the parent adducts.

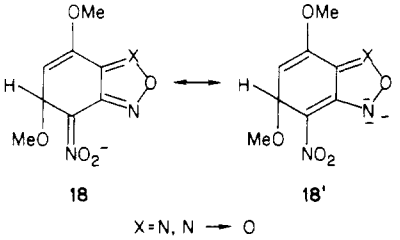

18 **18′**

X=N, N → O

Protonation at the para nitro group of some trinitrobenzene σ-complexes has been previously reported.[28-30] Typical examples are the nitronic acids $\mathbf{19aH^+}$–$\mathbf{dH^+}$, which have been characterized by NMR. Interestingly, the

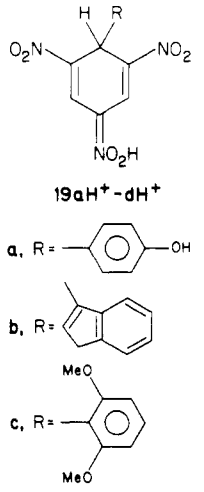

equilibrium formation of $\mathbf{19aH^+}$ from the parent phenoxide adduct has been spectrophotometrically studied and pK_a values of −1 and +3 have been measured for the ionization of $\mathbf{19aH^+}$ in aqueous and ethanolic solutions, respectively.[30] Since the acidity of oxygen acids usually decreases on going from water to methanol to ethanol,[31] these results suggest a pK_a value of ~1–2 for nitronic acids of the type $\mathbf{19H^+}$ and therefore for the nitronic acid $\mathbf{10H^+}$ of the picryl spiro adduct **10**. This estimation is indeed entirely consistent with the inobservation of $\mathbf{10H^+}$ under the experimental conditions, where the acid-catalyzed decomposition of **10** can be studied by stopped flow, i.e., pH >3.48. That the picryl nitronic acids are more acidic than the mononitrobenzofurazan and -benzofuroxan analogues by a factor of ~100 is probably due to the fact that part of the negative charge of the parent adducts is delocalized onto the two *o*-NO_2 groups, at least in solution.

Buffer Catalysis. The finding that the decompositon of **8a**, **8b**, and **10** is general acid catalyzed in methanolic solution is consistent with the results obtained for a number of spiro adducts in aqueous solution.[7,10,32,33] The statistically corrected Brønsted plots shown in Figure 6 yield α values of 0.56, 0.49, and 0.58 for the decomposition of **8a**, **8b**, and **10**, respectively. Such median α values are typical for a concerted acid catalysis with a transition state like **20**.[32-35] Also to be noted is that the noncatalyzed

(25) (a) Gripper Gray, A. C. Ph.D. Thesis, University of East Anglia, Norwich, England, 1966. (b) Boulton, A. J.; Gripper Gray, A. C.; Katritzky, A. R. *J. Chem. Soc. B* **1967**, 911.
(26) Strauss, M. J. *Chem. Rev.* **1970**, *70*, 667.
(27) Dalmonte, D.; Sandri, E.; Di Nunno, L; Florio, S.; Todesco, P. E. *J. Chem. Soc. B* **1971**, 2209.
(28) Wennerstrom, O. *Acta Chem. Scand.* **1971**, *25*, 2341.
(29) Moberg, C.; Wennerstrom, O. *Acta Chem. Scand.* **1971**, *25*, 2871.
(30) Buncel, E.; Eggimann, W. *Can. J. Chem.* **1976**, *54*, 2436.
(31) King, E. J. "Physical Chemistry of Organic Solvent Systems"; Covington, A. K., Dickinson, T., Eds.; Plenum Press: London, 1973; p 344.
(32) Bernasconi, C. F.; Gehriger, C. L.; de Rossi, R. H. *J. Am. Chem. Soc.* **1976**, *98*, 8451.
(33) Bernasconi, C. F.; Howard, K. *J. Am. Chem. Soc.* **1983**, *105*, 4690.
(34) Jencks, W. P. *Acc. Chem. Res.* **1976**, *9*, 425.
(35) Bernasconi, C. F.; Gandler, J. R. *J. Am. Chem. Soc.* **1978**, *100*, 8117.

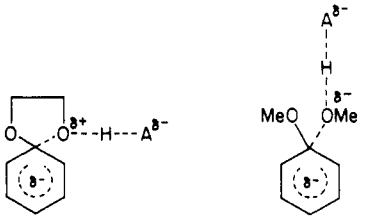

20 21

decomposition of the adducts does not occur via **20** (A = OMe). Should methanol act as a general acid in this process, the $k_{-2}/24.7$ values should fit the Brønsted plots of Figure 6 and be equal to about 2.4×10^{-5}, 4.5×10^{-7}, and 1.5×10^{-6} L mol^{-1} s^{-1} for **8a**, **8b**, and **10**, respectively. Instead, the experimentally found $k_{-2}/24.7$ values are equal to 0.085, 2.55×10^{-4}, and 1.01×10^{-3} L mol^{-1} s^{-1}. Thus, the noncatalyzed decomposition of the three spiro adducts studied is certainly a unimolecular reaction.

In contrast with that of **8a** and **8b**, the decomposition of the *gem*-dimethoxy adducts **6a** and **6b** was not found to be general acid catalyzed. This confirms recent observations by Bernasconi that catalysis of the decomposition of such adducts by carboxylic acids is generally weak and hardly detectable.[35] However, some catalysis of this process was observed in using cationic catalysts like pyridinium ions.[35] On this basis, the different behavior of spiro and *gem*-dimethoxy adducts was interpreted in terms of electrostatic effects arising from a different balance in the degree of proton transfer and C–O bond breaking in the transition states for acid decomposition of these complexes.[33] Thus, the experimental observations suggest substantial positive charge development on the departing oxygen atom in the transition state for the spiro adduct systems, as visualized in **20**, but either very little charge or some negative charge on the departing oxygen in the transition state for the dimethoxy adduct systems, as shown in **21**.[33] As a consequence, carboxylic acids may be effective catalysts in the case of the spiro adducts but not in that of the dimethoxy adducts. For these latter systems, the opposite situation prevails, and it is the cationic catalysts which will be more efficient.[33] The occurrence of these electrostatic interactions are of interest in that they provide indirect support to our proposal (vide supra) that the origin of the abnormal behavior of the benzofuroxan spiro adduct **8b** relative to its benzofurazan analogue **8a** must be understood in terms of electrostatic transition-state destabilization.

Experimental Section

Materials. 7-(2-Hydroxyethoxy)-4-nitrobenzofurazan (**7a**) and -benzofuroxan (**7b**) were prepared as previously described: **7a**, mp 115 °C; **7b**, mp 124 °C.[10] 4-Methoxy-7-nitrobenzofurazan (**4a**) and -benzofuroxan (**4b**) were also obtained according to literature procedures: **4a**, mp 116 ° (lit. mp 115–116 °C);[2b,36] **4b**, mp 162 °C (lit. mp 160–163 °C).[2a,37]

Methanolic benzenesulfonic acid and potassium methoxide solutions were prepared as previously described.[5] Buffer solutions were made up from the best available commercial grades of reagents, which were recrystallized or distilled before use.

Rate and pH Measurements. Stopped-flow determinations were performed on a Durrum stopped-flow spectrophotometer, the cell compartment of which was maintained at 20 ± 0.2 °C. All kinetic runs were carried out in triplicate with a substrate concentration in the range 3–5 × 10^{-5} M. Observed pseudo-first-order rate constants are accurate to ±3%.

The pH values were measured with a Tacussel Isis 2000 pH meter and are relative to the standard rate in pure methanol.

Registry No. **4a**, 18333-73-8; **4b**, 18378-09-1; **6a**, 64882-54-8; **6b**, 63153-26-4; **7a**, 66770-00-1; **7b**, 66770-02-3; **8a**, 98540-90-0; **8b**, 98540-91-1; **9**, 6478-31-5; **10**, 54846-61-6.

Supplementary Material Available: Tables of first-order rate constants for the formation and decomposition of **6a**, **6b**, **8a**, **8b**, and **10**, representative oscilloscope traces illustrating the decomposition of **8b**, an illustration of the effect of [$CHCl_2COOH$] on k_{obsd} for **8b**, and the UV–vis spectra for **4a**, **4b**, **6a**, **6b**, **6aH**$^+$, and **6bH**$^+$ (6 pages). Ordering information is given on any current masthead page.

(36) Dal Monte, D.; Sandri, E.; Mazzaracchio P. *Boll. Sci. Fac. Chim. Ind. Bologna* **1968**, *26*, 165.
(37) Ghosh, P. B.; Whitehouse, M. W. *J. Med. Chem.* **1968**, *11*, 305 and references therein.

Decomposition Reactions of a Cis-Diacyl Diimide. 4-Phenyl-1,2,4-triazoline-3,5-dione[1]

Robert A. Izydore,* Harriette E. Johnson, and Ronald T. Horton

Department of Chemistry, North Carolina Central University, Durham, North Carolina 27707

Received October 26, 1984

The cis-diacyl diimide 4-phenyl-1,2,4-triazoline-3,5-dione (**1**) was decomposed in a variety of solvent systems. In nonnucleophilic solvents under 80 °C **1** underwent nitrogen evolution and was converted to 2,6-diphenyltriazolo[1,2-*a*]-*s*-triazole-1,3,5,7-tetrone (**2**). At higher temperatures **1** gave phenyl isocyanate (**3**). In nucleophilic solvent systems (acetic acid, alcohols, or water) **1** underwent loss of nitrogen and formed mixtures containing varying amounts of **2**, 1-(*N*-phenylcarbamoyl)-4-phenylurazole (**5**), 4-phenylurazole (**11**), diphenylurea (**12**), *N*-phenylcarbamates (**13**), and 1-(alkoxycarbonyl)-4-phenylurazoles (**14**), depending on the decomposition conditions employed. The mechanistic pathways leading to the various products are discussed.

Cis-diacyl diimides are cyclic electron-deficient azo compounds that react readily with olefinic and acetylenic sites. As such they have been employed as intermediates in the synthesis of a wide variety of heterocyclic systems. They are in general unstable compounds and often must be generated and trapped in solution at low temperatures. The 4-substituted triazoline-3,5-diones, often referred to as RTAD, are the most extensively utilized derivatives of this class of compounds principally because of their high reactivity and the fact that they can be isolated and stored under inert conditions.[2,3] When subjected to thermolysis,

(1) (a) Presented in part at the 181st National Meeting of the American Chemical Society, Atlanta, GA, April 1980; ORGN 178. (b) Presented in part at the 189th National Meeting of the American Chemical Society, Miami Beach, FL, May 1985; ORGN 116.

(2) Cookson, R. C.; Gupte, S. S.; Stevens, I. D. R.; Watts, C. T. "Organic Syntheses"; Wiley: New York, 1971; Vol. 51, p 121.

0022-3263/85/1950-4589$01.50/0